Microwave-Assisted Growth and Characterization of Water-Dispersed CdTe/CdS Core−Shell Nanocrystals with High Photoluminescence

Yao He,[§] Hao-Ting Lu,[§] Li-Man Sai,[§] Wen-Yong Lai,[§] Qu-Li Fan,[§,||] Lian-Hui Wang,*[,‡,§] and Wei Huang*[,†,§,||,⊥]

Institute of Advanced Materials (IAM), Fudan University, 220 Handan Road, Shanghai 200433, People's Republic of China, Institute of Advanced Materials (IAM), Nanjing University, 22 Hankou Road, Nanjing 210093, People's Republic of China, and Department of Engineering, National University of Singapore, 9 Engineering Drive 1, Singapore 117576, Republic of Singapore

Received: December 23, 2005; In Final Form: May 9, 2006

A novel microwave-assisted method of growth of high-quality CdTe/CdS core−shell nanocrystals in the aqueous phase is presented in this paper. The photoluminescence quantum yield (PLQY) is greatly enhanced by epitaxial growth of the CdS shell. Under optimum conditions, the PLQY of as-prepared nanocrystals reaches as high as 75% without any post-treatment. Furthermore, these investigations demonstrate that microwave irradiation is tremendously useful for fast epitaxial growth of nanocrystals due to its special characteristics. As a result, the microwave synthesis is sufficiently time-economizing (only five minutes are required) to obtain optimum amounts of CdTe/CdS core−shell nanocrystals in comparison to the conventional illumination method (several days are required). Therefore, this current research not only provides a rapid microwave synthesis for producing highly fluorescent CdTe/CdS core−shell nanocrystals, but also it presents some advantages of the microwave synthesis in comparison to the illumination method.

1. Introduction

Semiconductor nanocrystals (NCs) have attracted tremendous attention with both theoretical studies and practical applications due to their unique electrical and optical properties.[1,2] The conjugation of semiconductor nanocrystals with biomolecules became an increasingly attractive research area after water-dispersed nanocrystals were successfully applied for biological labeling in 1998.[3,4] Tremendous progress in biological applications of nanocrystals has been achieved during these years.[5−7] Obviously, water-dispersed nanocrystals with good spectral properties play a critical role in biological applications such as fluorescent labeling.[8] Although nanocrystals with a high photoluminescence quantum yield (PLQY) were obtained through the TOP/TOPO organometallic synthetic approach,[9−11] their hydrophobic character rendered them unsuitable for direct use in biological systems. Polymer coating is an effective approach to disperse as-prepared nanocrystals in water, which has been commercialized by the Quantum Dots Corporation. In brief, the hydrophobic nanocrystals are covered with a hydrophilic polymer shell by interactions between the polymer and the nanocrystal surfactant molecules. Thus, the nanocrystals become soluble in water.[12] Although this technique is efficient, it is relatively complicated and requires additional steps. Another main method is to substitute the hydrophilic molecules, which have strong polar groups such as carboxylic acid or reactive groups such as Si−O−R,[13] for surface-binding TOPO. However, the PLQY often decreases when the nanocrystals are transferred into water because the polarity of water is too strong to disrupt various equilibria related to the nanocrystals.[14,15]

Direct synthesis of nanocrystals in the aqueous phase is an alternative strategy to obtain water-dispersed nanocrystals. However, nanocrystals synthesized in the aqueous phase often have poor spectral properties (relatively low PLQY ∼ 3−10% and broad full width at half-maximum (fwhm)). In addition, a long reaction time (from several hours to several days) was required in conventional aqueous synthesis.[16] Systematic investigations reveal that a high concentration of surface defects of nanocrystals leads to low PLQY.[17,18] To optimize the spectral properties of water-dispersed nanocrystals, different strategies have been developed since the first report on aqueous synthesis of 3-mercapto-1,2-propanediol-capped CdTe nanocrystals in 1993.[19] One strategy is to synthesize nanocrystals at a higher temperature, which is available for accelerating the growth rate and reducing the concentration of surface defects. For example, CdTe nanocrystals synthesized at 180 °C in the aqueous phase by a hydrothermal method possessed excellent quality and were directly used as biological labels.[20] In addition, although the detailed interpretation about microwave irradiation greatly enhancing the quality of nanocrystals has not been depicted up to the present, water-dispersed CdTe nanocrystals whose PLQY reached 60% in the optimum case were successfully obtained via microwave irradiation.[21]

On the other hand, it has been demonstrated that epitaxial growth of a shell with broader band gap on the surface of fluorescent nanocrystals is an effective approach to improve the spectral properties of nanocrystals. The reason is that the shell can provide a passivation of the nanocrystals surface, which can reduce surface nonradiative recombination defects effectively and lead to enhancement of PLQY.[22] Many successful systems of core−shell nanocrystals were achieved through an organometallic route.[23−25] However, there are only a few

* Corresponding authors.
† Telephone: +86-21-5566-4188/4198. Fax: +86-21-6565-5123/5566-4198. E-mails: wei-huang@fudan.edu.cn and chehw@nus.edu.sg.
‡ E-mail: wlhui@fudan.edu.cn.
§ Fudan University.
|| Nanjing University.
⊥ National University of Singapore.

10.1021/jp057498h CCC: $33.50 © 2006 American Chemical Society
Published on Web 06/21/2006

successful examples toward the core−shell structure obtained in aqueous systems (citrate-stabilized CdSe/CdS nanocrystals[26] and thioglycolic acid (TGA)-stabilized CdTe/CdS nanocrystals[15]). In detail, citrate-stabilized CdSe nanocrystals or TGA-stabilized CdTe nanocrystals were exposed under ambient light to realize formation of the CdS shell through photodegradation of the stabilizer. Both of the as-prepared core−shell nanocrystals possessed high PLQY because the CdS shell provided a passivation of the core nanocrystal surface, which effectively smoothed the surface and reduced surface traps of core nanocrystals. However, the procedure was sufficiently time-consuming (5 days or 20 days were required to obtain citrate-stabilized CdSe/CdS nanocrystals or TGA-stabilized CdTe/CdS nanocrystals with the highest PLQY, respectively), since it required gradual and slow photooxidation of TGA to the form CdS shell. Moreover, broad fwhm was observed due to the wide size distribution of nanocrystals, which resulted from a long reaction time. In addition, CdTe nanocrystals capped with other thiols such as 3-mercaptopropionic acid (MPA) were not available for forming a core−shell system, since MPA did not produce sulfide ions through photodegradation.

To overcome the deficiency of the illumination method applied for synthesizing nanocrystals with core−shell structure, we here demonstrate a novel microwave synthesis of highly luminescent CdTe/CdS core−shell nanocrystals stabilized with MPA in the aqueous phase. The as-prepared CdTe/CdS core−shell nanocrystals obtained without any post-preparative treatment possessed high PLQY (∼75%) and narrow size distribution (fwhm ∼ 35 nm). Furthermore, some advantages of the microwave synthesis in comparison to the illumination method were discussed as well.

2. Experiment Section

2.1. Materials. Tellurium powder (99.9%) and $CdCl_2$ (99.9%) were purchased from Aldrich. 3-Mercaptopropionic acid (MPA) (98%) was purchased from Fluka. $NaBH_4$ (99%) and Na_2S (99%) were obtained from Shanghai Chemical Reagents Company. All chemicals were used without additional purification. All solutions were prepared using Milli-Q water (Millipore) as the solvent.

2.2. Preparation of NCs. *2.2.1. Preparation of CdTe Core NCs.* Nearly monodisperse CdTe core NCs were obtained via microwave irradiation as described previously.[21] Briefly, the CdTe precursor solution was prepared by adding freshly prepared NaHTe solution to a N_2-saturated $CdCl_2$ solution at pH 8.4 in the presence of 3-mercaptopropionic acid (MPA) as stabilizer. The precursor concentrations were [Cd] = 1.25 mmol/L, [MPA] = 3.0 mmol/L, [Te] = 0.625 mmol/L, respectively. An amount of 50 mL of CdTe precursor solution was injected into the exclusive vitreous vessel. CdTe NCs with the maximum emission wavelength of around 520 nm were prepared under micorwave irradiation for 1 min at 100 °C. The CdTe NCs sample was taken when the temperature decreased naturally to lower than 50 °C. The as-prepared CdTe solution was concentrated by 4 times and was then precipitated with 2-propanol by centrifugation. The colloidal precipitate was redissolved in 3 mL of ultrapure water, acting as CdTe core NCs.

2.2.2. Preparation of CdTe/CdS Core−Shell NCs. The CdTe/CdS precursor solution was prepared by adding the as-prepared CdTe core NCs to a N_2-saturated solution with the concentration of 1.25 mmol/L $CdCl_2$, 1.0 mmol/L Na_2S, and 6.0 mmol/L MPA in pH 8.4. An amount of 4 mL of CdTe/CdS precursor solution was injected into the exclusive vitreous vessel. Serial sizes of high-quality CdTe NCs were achieved on the basis of regulating the reaction time of microwave irradiation. After finishing microwave irradiation, the CdTe/CdS NCs sample was taken when the temperature decreased naturally to lower than 50 °C. No post-preparative treatment was performed on any of the samples for optical characterizations. Samples were precipitated by 2-propanol and dried in a vacuum oven for XRD and XPS characterization. TEM, HRTEM, and EDAX samples were prepared by dropping the aqueous CdTe/CdS solution onto carbon-coated copper grids with the excessive solvent evaporated. The PLQY at room temperature was estimated using R6G (QY = 95%), R640 (QY = 100%), or LD690 (QY = 63%) in ethanol, respectively, according to the different maximum emission wavelengths of CdTe/CdS core−shell NCs.[10,27]

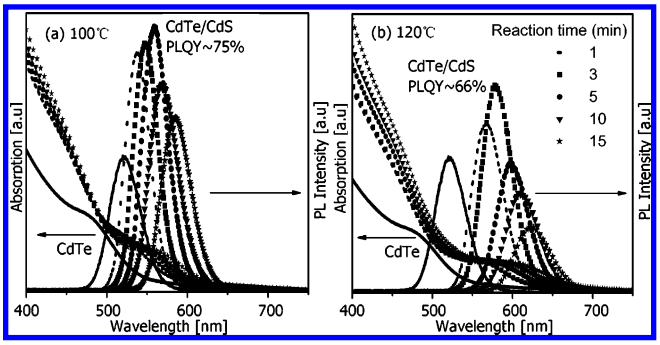

Figure 1. (a), (b) Temporal evolution of absorption and corresponding PL spectra of CdTe/CdS NCs prepared at different temperatures and time. Spectra of CdTe cores and CdTe/CdS NCs are shown with solid lines and symbols as indicated in the figure, respectively.

2.3. Apparatus. The microwave system (Discover Application Software Version 3.5.7) used for synthesizing CdTe/CdS core−shell NCs was made by CEM of America. The system operates at 2450-MHz frequency, and works at 0∼300-W power. Exclusive vitreous vessels with a volume of 10 or 100 mL are equipped for the system to provide security during reaction demanding high temperature and pressure. UV−vis absorption spectra were obtained using a Shimadzu UV-3150 UV−vis−near-infrared spectrophotometer. Fluorescence experiments were performed using a Shimadzu RF-6301PC spectrofluorimeter. All optical measurements were performed at room temperature under ambient conditions. The XRD patterns were obtained from a Rigaku D/max-gB diffractometer. XPS was carried out using Microlab 310F. EDAX, TEM, and HRTEM overview images were recorded on a JEOL JEM 2011 electron microscope operated at 200 kV.

3. Results and Discussion

3.1. Characterization. Figure 1, parts a and b, displays the UV−vis absorption and photoluminescence (PL) spectra of CdTe/CdS core−shell NCs synthesized through microwave irradiation at 100 and 120 °C, respectively. A significant red-shift was observed in both the absorption and PL spectra of CdTe/CdS NCs in contrast to those of CdTe NCs. This was an indication of the formation of a CdTe/CdS core−shell structure rather than a $CdTe_xS_{1-x}$ alloyed structure. The reason was that the formation of $CdTe_xS_{1-x}$ alloyed NCs would lead to a blue-shift in the absorption and PL spectra due to the larger band-gap energy of $CdTe_xS_{1-x}$ alloyed NCs in comparison to pure CdTe NCs.[28,29] The thickness of the CdS shell increased with prolonging reaction time, which resulted in a gradual red-shift. The red-shift along with shell growth was the result of a decrease of the kinetic energy of the excited electron and a hole in the NCs because of the spreading of their wave functions into the shell.[30] In the presence of CdTe NCs and excessive cadmium

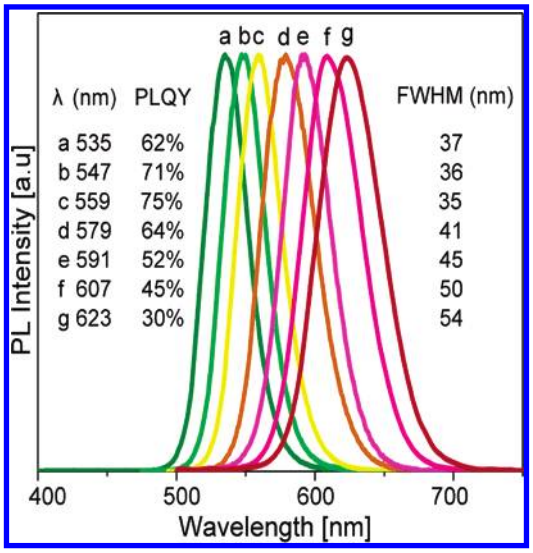

Figure 2. PL spectra of CdTe/CdS NCs with serial maximum emission wavelength, and related PLQY and fwhm values are presented.

ions in the system, sulfide ions reacted with cadmium ions on the CdTe NCs surface and formed a shell structure of CdS, whose band gap was larger than that of CdTe.[15] A large amount of surface traps of CdTe NCs were effectively eliminated due to formation of a CdS shell, leading to a tremendous enhancement in PL intensity.[15,26] The PL intensity reached the maximum value in the case in which the thickness of CdS shell increased to a critical threshold (the optimum thickness). Afterward, the PL intensity declined while continuing to prolong the reaction time. The reason was that dislocations and new defects formed as the thickness of the CdS shell increased unceasingly, which resulted from the intrinsic strains due to the lattice mismatch (11.5%) between CdTe and CdS.[28,29] As a result, these defects became a new source of nonradiative recombination sites and the PL intensity decreased again.[31]

The temperature was extraordinarily critical during the process of forming a CdS shell on CdTe cores. As shown in Figure 1, the maximum PL intensity could be achieved while the reaction time reached 5 min (100 °C as reaction temperature) or 3 min (120 °C as reaction temperature), respectively. We deduced that less time was demanded to form the CdS shell with the optimum thickness corresponding to higher temperature because the rate of epitaxial growth was markedly accelerated at higher temperature.[31] However, the CdTe seeds commenced growing via Ostwald ripening, and their size distribution deteriorated at higher temperatures (120 °C) in the meantime. By contrast, a CdS shell with a high degree of crystallinity was obtained and the steady epitaxial growth of the CdS shell could be preserved at 100 °C, which was favorable for the formation of uniform CdTe/CdS core−shell NCs.[17] Therefore, relatively better spectral properties (PLQY ∼ 60−75%, fwhm ∼ 35−45 nm) can be achieved at 100 °C compared to 120 °C (PLQY ∼ 45−66%, fwhm ∼ 45−55 nm). In addition, a lower temperature (80 or 90 °C) was also selected as the reaction temperature. Poor-quality CdTe/CdS core−shell NCs were obtained because of incomplete decomposition of the precursors and low crystalline degree of the CdS shell at lower temperature.[28,29]

Figure 2 displays the normalized PL spectra of the CdTe/CdS NCs with different maximum emission wavelengths in aqueous solution, corresponding to the change of wavelength from 535 to 623 nm. Compared with CdTe core NCs (PLQY ∼ 40%), the PLQY of CdTe/CdS core−shell NCs was tremendously enhanced and reached as high as 75% in optimum

Figure 3. Photograph of the wide spectral range of bright luminescence from a sample of CdTe/CdS NCs aqueous solution without any post-preparative treatment under irradiation with 365-nm ultraviolet light from a UV lamp.

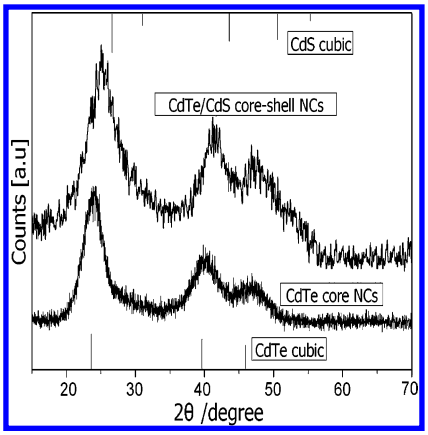

Figure 4. XRD patterns of both CdTe core NCs and the corresponding CdTe/CdS core−shell NCs. The standard diffraction lines of cubic CdTe and cubic CdS are also shown for comparison.

conditions. In addition, Figure 3 shows the wide spectral range of highly luminescent CdTe/CdS NCs dispersed in water. As the thickness of CdS shell increased, the luminescent color displayed a continuous diversification from green, yellow, orange, to red.

The powder XRD patterns recorded from both the CdTe and CdTe/CdS solid samples precipitated from aqueous solution with an excess of 2-propanol are shown in Figure 4. The diffraction of bare CdTe NCs is quite close to that for bulk cubic CdTe. By contrast, the diffraction pattern of CdTe/CdS NCs moves slightly toward a higher angle due to formation of the CdS shell on CdTe core NCs.[15] In addition, the pattern of peak widths and shapes is nearly unchanged, which further demonstrates the formation of the CdS/CdTe core−shell structure rather than $CdTe_xS_{1-x}$ alloyed structure. The reason is that a homogeneous alloy would show a significant narrowing of XRD peak widths with increasing size.[30] The distribution of bond lengths resulting from intrinsic strains is a possible explanation for why XRD peak widths and shapes of core/shell NCs are approximate with those of the core NCs.[30] Similar changes in diffraction pattern are consistent with previous reports as well.[31,32]

On the other hand, X-ray photoelectron spectroscopy (XPS) provides available evidence for the epitaxial growth of the CdS shell on CdTe core NCs. The XPS spectra of S2p recorded from CdTe core NCs and the corresponding CdTe/CdS core−shell NCs are presented in Figure 5. The binding energy (163.6 eV) of S2p from CdTe NCs demonstrates the existence of chemical bonds (Cd−SR) between thiols and cadmium ions on the surface

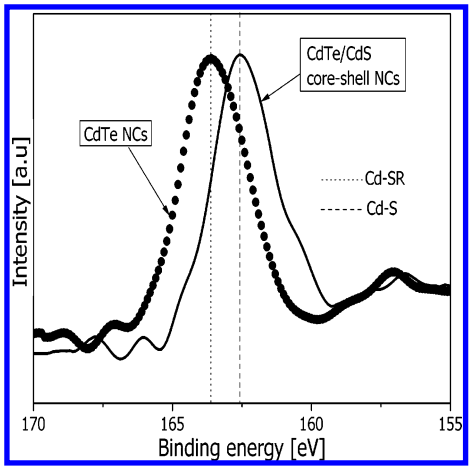

Figure 5. XPS spectra of S2p recorded from CdTe core NCs and the corresponding CdTe/CdS core−shell NCs. The vertical lines are guides for positions of S2p from Cd−MAP (SR) and Cd−S, respectively. Their positions are 163.6 eV (Cd−SR) and 162.7 eV (Cd−S), respectively.

of CdTe NCs.[17] Compared with CdTe NCs, the binding energy (162.7 eV) of S2p from CdTe/CdS core−shell NCs shifts to lower energy, indicating that the coordination situation of S from CdTe/CdS NCs is different with that of Cd−SR. As a result, the new S2p can be attributed to the S from CdS;[15,29] it can therefore further confirm the proposed core−shell structure in which CdS acts as a shell encapsulating the CdTe core.

Figure 6 shows transmission electron microscopy (TEM) and high resolution of transmission electron microscopy (HRTEM) overview images of the as-prepared CdTe/CdS core−shell NCs and the size distributions. Under TEM, the as-prepared CdTe/CdS NCs appear as spherical particles with crystalline structures and possess excellent monodispersity. The existence of well-resolved lattice planes on the HRTEM image further confirms the crystalline structure of as-prepared CdTe/CdS NCs. In addition, The lattices stretch straight across entire nanocrystals with no evidence of an interface, which is consistent with a coherent epitaxial mechanism for the growth and indicates that the increase of particle size does not disturb their crystalline form.[28,31] The size distribution was determined by measuring more than 200 particles, which also reveals the excellent monodispersity of the sample. Furthermore, in comparison with the core size of 2.2 nm,[16,33] the size of CdTe/CdS NCs increases to 4.1 nm, which indicates that the optimal thickness of the CdS shell is 1.9 nm. In addition, energy-dispersive X-ray analysis (EDAX) measurements clearly show the presence of cadmium, tellurium, and sulfur in thoroughly washed highly luminescent nanocrystals.

3.2. Illumination Method and Microwave Synthesis of CdTe/CdS Core−Shell NCs. As mentioned in ref 15, TGA-stabilized CdTe nanocrystals were exposed under ambient light to realize formation of the CdS shell through photodegradation of the stabilizer. The as-prepared core−shell nanocrystals possessed high PLQY because the CdS shell provided a passivation of the core nanocrystals surface, which effectively smoothed the surface and reduced surface traps of core nanocrystals. However, the procedure was sufficiently time-consuming, and more than 20 days were required to obtain TGA-stabilized CdTe/CdS nanocrystals with the highest PLQY; the reason was that it required gradual and slow photooxidation of TGA to form the CdS shell. Moreover, broad fwhm was observed due to the wide size distribution of nanocrystals. In addition, CdTe nanocrystals stabilized with 3-mercaptopropionic acid (MPA) were not available for forming a core−shell system because MPA did not produce sulfide ions through photodegradation. Similar explanations were discussed in the citrate-stabilized CdSe/CdS core−shell system.[26]

By contrast, microwave irradiation can heat up the aqueous solution homogeneously due to the penetration characteristic of microwaves, which is an essential prerequisite to the formation of monodispersed nanoparticles.[34] On the other hand, microwaves can penetrate the reaction solution leading to simultaneous fast heating, and the temperature can be raised rapidly due to the high utilization factor of microwave energy.[35,36] Thus, as mentioned above, the successive process of CdS shell growth by epitaxy can be realized to form CdTe/CdS core−shell nanocrystals in an extremely short period of time, which is extraordinarily beneficial for accelerating the growth rate and reducing the concentration of surface defects of nanocrystals.[20,21] Therefore, the microwave synthesis is sufficiently time-economizing in comparison to the illumination method. Furthermore, compared with only TGA being used as a stabilizer to synthesize CdTe/CdS core−shell nanocrystsals by the illumination method, the microwave synthesis can be applied for synthesizing CdTe/CdS core−shell nanocrystals capped with other thiols such as MPA, despite the fact that it does not produce sulfide ions through illumination.

4. Conclusion

In summary, a novel microwave synthesis of water-dispersed and highly luminescent CdTe/CdS core−shell nanocrystals is presented in this paper. This method allows the rapid synthesis of high-quality CdTe/CdS core−shell nanocrystals in moderate conditions in aqueous phase. Our results shown above demonstrated that the as-prepared CdTe/CdS core−shell nanocrystals

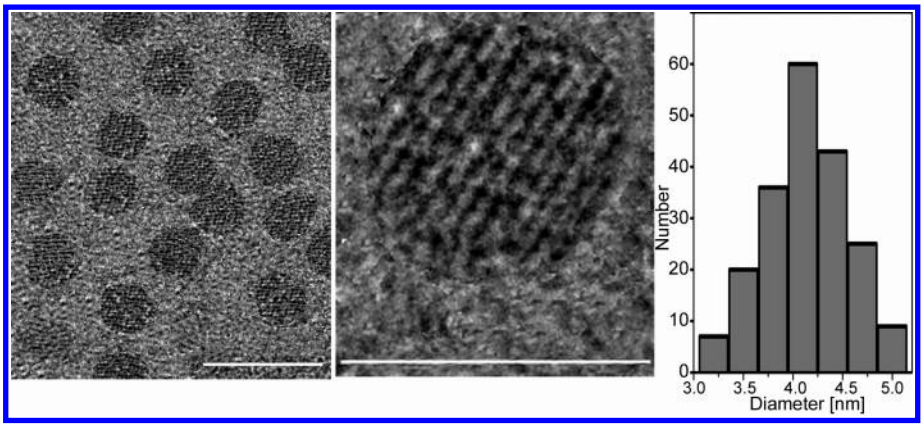

Figure 6. TEM (left) and HRTEM (middle) overview images of CdTe/CdS NCs synthesized through microwave irradiation, and the size distribution on the right. Scale bars are 10 nm (left) and 5 nm (middle), respectively.

without any post-preparative treatment possessed a high photoluminescence quantum yield (up to 75%) and a narrow size distribution (fwhm ~ 35 nm). More importantly, our investigations show that microwave irradiation is extremely suitable for accelerating epitaxial growth of CdS shell. As a result, merely 5 minutes were required to form an optimum thickness of the CdS shell in the microwave synthesis compared with several days expended in the illumination method. Moreover, in comparison to TGA exclusively being available for synthesizing CdTe/CdS core−shell nanocrystals in the illumination method, the microwave synthesis can be applied for synthesizing core−shell nanocrystals capped with other thiols such as MPA. Furthermore, the microwave synthesis is extremely simple and convenient and free of complicated vacuum manipulation or expensive chemical reagents. In addition, it is also environmentally and biologically friendly since the whole synthesis is carried out in water. Therefore, we consider thus novel method as an important step to rapidly prepare water-dispersed and highly luminescent CdTe/CdS core−shell nanocrystals. We are currently investigating the microwave synthesis of others kinds of core−shell nanocrystals, which can be potentially used for biolabeling and a great variety of bio-imaging purposes; the further outcomes will be presented in future papers.

Acknowledgment. This work was financially supported by the National Natural Science Foundation of China under Grants 90406021, 50428303, and 30425020, as well as the Shanghai Commission of Education under Grant 2004SG06.

References and Notes

(1) Rogach, A. L.; Katsikas, L.; Kornowski, A.; Su, D. S.; Eychmuller, A.; Weller, H. *Ber. Bunsen-Ges. Phys. Chem.* **1996**, *100*, 1772−1778.

(2) Gaponenko, S. V. *Optical Properties of Semiconductor Nanocrystals*; Cambridge University Press: Cambridge, 1998.

(3) Bruchez, M. P.; Moronne, M.; Gin, P.; Weiss, S.; Alivisatos, A. P. *Science* **1998**, *281*, 2013−2016.

(4) Chan, W. C. W.; Nie, S. *Science* **1998**, *281*, 2016−2018.

(5) Parak, W. J.; Gerion, D.; Pellegrino, T.; Zanchet, D.; Micheel, C.; Williams, S. C.; Boudreau, R.; Gros, M. A. L.; Larabell, C. A.; Alivisatos, A. P. *Nanotech* **2003**, *14*, 15−27.

(6) Gao, X.; Cui, Y. Y.; Levenson, R. M.; Chung, L. W. K.; Nie, S. *Nat. Biotech.* **2004**, *22*, 969−976.

(7) Katz, E.; Willner, I. *Angew. Chem., Int. Ed.* **2004**, *43*, 6042−6108.

(8) Michalet, X.; Pinaud, F. F.; Bentolila, L. A.; Tsay, J. M.; Doose, S.; Li, J. J.; Sundaresan, G.; Wu, A. M.; Gambhir, S. S.; Weiss, S. *Science* **2005**, *307*, 538−544.

(9) Talapin, D. V.; Haubold, S.; Rogach, A. L.; Kornowski, A.; Haase, M.; Weller, H. *J. Phys. Chem. B* **2001**, *105*, 2260−2263.

(10) Qu, L.; Peng, X. *J. Am. Chem. Soc.* **2002**, *124*, 2049−2055.

(11) Yu, W.; Wang, A.; Peng, X. *Chem. Mater.* **2003**, *15*, 4300−4308.

(12) Pellegrino, T.; Manna, L.; Kudera, S.; Liedl, T.; Koktysh, D.; Rogach, A. L.; Keller, S.; Radler, J.; Natile, G.; Parak, W. J. *Nano Lett.* **2004**, *4*, 703−707.

(13) Gerion, D.; Pinaud, F.; Williams, S. C.; Parak, W. J.; Zanchet, D.; Weiss, S.; Alivisatos, A. P. *J. Phys. Chem. B* **2001**, *105*, 8861−8871.

(14) Wuister, S. F.; Swart, I.; Driel, F. V.; Hickey, S. G.; Donega, C. M. *Nano Lett.* **2003**, *3*, 503−507.

(15) Bao, H.; Gong, Y.; Li, Z.; Gao, M. *Chem. Mater.* **2004**, *16*, 3853−3859.

(16) Gaponik, N.; Talapin, D.; Rogach, A. L.; Hoppe, K.; Shevchenko, E.; Kornowski, A.; Eychmuller, A.; Weller, H. *J. Phys. Chem. B* **2002**, *106*, 7177−7185.

(17) Borchet, H.; Talapin, D. V.; Gaponik, N.; McGinley, C.; Adam, S.; Lobo, A.; Moller, T.; Weller, H. *J. Phys. Chem. B* **2003**, *107*, 9662−9668.

(18) Crisp, M. T.; Kotov, N. A. *Nano Lett.* **2003**, *3*, 173−177.

(19) Rajh, T.; Micic, O.; Nozik, A. *J. Phys. Chem. B* **1993**, *97*, 11999−12003.

(20) Zhang, H.; Wang, L.; Xiong, H.; Hu, L.; Yang, B.; Li, W. *Adv. Mater.* **2003**, *15*, 1712−1715.

(21) Li, L.; Qian, H.; Ren, J. *Chem. Commun.* **2005**, 528−530.

(22) Radtchenko, I. L.; Sukhorukov, G. B.; Gaponik, N.; Kornowski, A.; Rogach, A. L.; Mohwald, H. *Adv. Mater.* **2001**, *13*, 1684−1687.

(23) Hao, E.; Sun, H.; Zhou, Z.; Liu, J.; Yang, B.; Shen, J. *Chem. Mater.* **1999**, *11*, 3096−3102.

(24) Li, J.; Wang, A.; Guo, W.; Keay, J.; Mishima, T.; Johnson, M.; Peng, X. *J. Am. Chem. Soc.* **2003**, *125*, 12567−12575.

(25) Tsay, J. M.; Pflughoefft, M.; Bentolila, L. A.; Weiss, S. *J. Am. Chem. Soc.* **2004**, *126*, 1926−1927.

(26) Wang, Y.; Tang, Z.; Correa-Duarte, M. A.; Pastoriza-Santos, I.; Giersig, M.; Kotov, N. A.; Liz-Marzan, L. M. *J. Phys. Chem. B* **2004**, *108*, 15461−15469.

(27) Grosby, G. A.; Demas, J. N. *J. Phys. Chem.* **1971**, *75*, 991−1024.

(28) Mekis, I.; Talapin, D. V.; Kornowski, A.; Haase, M.; Weller, H. *J. Phys. Chem. B* **2003**, *107*, 7454−7462.

(29) Pan, D.; Wang, Q.; Jiang, S.; Ji, X.; An, L. *Adv. Mater.* **2005**, *17*, 176−179.

(30) Peng, X.; Schlamp, M.; Kadavanich, A. V.; Alivisatos, A. P. *J. Am. Chem. Soc.* **1997**, *119*, 7019−7029.

(31) Dabbousi, B. O.; Rodriguez-Viejo, J.; Mikulec, F. V.; Heine, J. R.; Mattoussi, H.; Ober, R.; Jensen, K. F.; Bawendi, M. G. *J. Phys. Chem. B* **1997**, *101*, 9463−9475.

(32) Harrison, M. T.; Kershaw, S. V.; Rogach, A. L.; Kornowski, A.; Eychmuller, A.; Weller, H. *Adv. Mater.* **2000**, *12*, 123−125.

(33) Yu, W. W.; Qu, L.; Guo, W.; Peng, X. *Chem. Mater.* **2003**, *15*, 2854−2860.

(34) Yin, H.; Yamanoto, T.; Wada, Y.; Yanagida, S. *Mater. Chem. Phys.* **2004**, *83*, 66−70.

(35) Komarneni, S.; Li, D.; Newalkar, B.; Katsuki, H.; Bhalla, A. S. *Langmuir* **2002**, *18*, 5959−5962.

(36) Chen, D.; Shen, G.; Tang, K.; Lei, S.; Zheng, H.; Qian, Y. *J. Cryst. Growth* **2004**, *260*, 469−474.